EXPERIMENTAL DATA ON STEAM BUBBLE CONDENSATION IN POLY-DISPERSED UPWARD VERTICAL PIPE FLOW

D. Lucas, M. Beyer, L. Szalinski

Forschungszentrum Dresden-Rossendorf e.V., Institute of Safety Research
P.O.Box 510 119, 01314 Dresden, Germany
Phone: +49 (0) 351 260 2047, Fax: +49 (0) 351 260 12047
D.Lucas@fzd.de

Abstract

Experiments were done at the TOPFLOW facility of the Forschungszentrum Dresden-Rossendorf to establish a CFD-grade database on the condensation of steam bubbles injected into sub-cooled upwards vertical pipe flow. Bubble condensation has to be considered in Nuclear Reactor Safety Research, e.g. if sub-cooled boiling or bubble entrainment caused by ECC injection occurs. Bubble size distributions are important, since the condensation rate is proportional to the interfacial area density. To develop and validate closure models for CFD codes experimental data with high resolution in space and time are required. The steam was injected via orifices in the pipe wall located at different distances from measuring plane. 1 mm and 4 mm injection orifices are used to vary the initial bubble size distribution. The variation of the distance between the location of the gas injection and the measuring plane allows investigating the evolution of the flow along the pipe. Pressure, steam and water flow rates and the sub-cooling were also varied. Measurements are done using wire-mesh sensors and thermocouples. Data on averaged void fraction, radial gas volume fraction profiles, profiles of the gas velocity and bubble size distributions in dependency of the L/D ratio are available.

1. INTRODUCTION

While CFD codes are frequently used for industrial applications on single phase flow problems they are not mature for two-phase flows. An overview on the present two-phase capabilities of CFD-Codes related to Nuclear Reactor Safety (NRS) Research is given by Bestion et al. (2009). The qualification of CFD codes for two-phase flows is one of important requirement of future NRS research. There are different ongoing activities worldwide to meet this goal. In frame of the German Computational Fluid Dynamic (CFD) association activities of different institutions are united to develop and validate CFD codes for their application to nuclear reactor safety assessment. The reference code chosen for this purpose is ANSYS-CFX, but the developed closure models are widely code independent. In the European frame the Integrated Project NURISP should be mentioned which aims on the establishment and further development of an European Code platform for NRS. In the sub-project on thermo-hydraulics the improvement of the two-phase capabilities of CFD codes is one of the most important topics.

Two-phase flows are characterized by a complex structure of the interfaces between the phases. As with turbulence, in general it will not be possible to resolve this interface in the numerical model with all its fine structures. Instead, averaging procedures are applied which blur the information on the interface. The widely used two-fluid model (see e.g. Drew and Lahey, 1979, Ishii and Mishima, 1984) assumes two interpenetrating phases – i.e. both phases are present simultaneously at each spatial location; just the volume fractions occupied by each of the phases are considered, and their variation in space and time. However, all interfacial transfers – mass, momentum and energy – sensitively depend on the interfacial structure. For this reason, these transfers have to be considered by closure models even in multi-phase CFD simulation.

The validation of CFD codes, modelling concepts and closure models requires the acquisition of new experimental data with a high resolution in space and time. New measurement techniques such as tomography methods have to be developed and applied to meet these requirements. The TOPFLOW facility of Forschungszentrum-Dresden-Rossendorf (FZD) combines two-phase flow experiments at

conditions close to the application (high pressure and temperature, relatively large scales) and innovative measuring techniques.

A special topic of our research is the development and validation of models for poly-dispersed flows. Many activities were done to improve the modelling of adiabatic bubbly flows in the frame of CFD. In this case models for momentum transfer between the phases are most important. Usually they are expressed as so-called bubble forces. Experimental investigation as well as Direct Numerical Simulations (DNS) showed, that these bubble forces strongly depend on the bubble size. In addition to the well known drag force also virtual mass, lift, turbulent dispersion and wall forces have to be considered (Lucas et al., 2007). The lift forces even changes its sign in dependence of the bubble size (Tomiyama et al., 2002). In consequence large bubbles are pushed to the opposite direction than small bubbles if a gradient of the liquid velocity perpendicular to the relative bubble velocity exists (Lucas et al., 2001, Prasser et al., 2007). To simulate the separation of small and large bubbles more than one momentum equation is required (Krepper et al., 2005). For this reason recently so-called Inhomogeneous-MUSIG (MUlti SIze Group) model was implemented into the ANSYS-CFX code (Frank et al., 2008, Krepper et al., 2008). It allows the consideration of a number of bubble classes independently for the mass balance (for a proper modelling of bubble coalescence and breakup a large number of bubble groups is required) and for the momentum balance (only very few classes can be considered due to the high computational effort, criteria for the classification can be derived from the dependency of the bubble forces on the bubble size, e.g. the change of the sign of the lift force). In the first version of the Inhomogeneous MUSIG model only transfers between the bubble classes due to bubble coalescence and breakup can be modelled. In case of flows with phase transfer additional transfers between the single classes and the liquid and transfers between bubble classes caused by growth or shrinking of bubbles have to be considered. The equations for the extension of the MUSIG models were derived (Lucas et al., 2009) and recently implemented into the CFX code.

These extensions of the Inhomogeneous MUSIG model allow to simulate flows with phase transfer in principle. However, for a simulation based on physics in addition proper closure models for evaporation and condensation rates are required. Usually these phase transfer rates are assumed to be proportional to the interfacial area density and the overheating or sub-cooling, respectively. For this reason detailed information on the evolution of local bubble size distributions and local temperature profiles is needed. Wire-mesh sensors were successfully used to measure local bubble size distributions in air-water (Lucas et al., 2010), steam-water (Prasser et al., 2007) and air-silicone oil (Szalinski et al., 2010) flows. Especially the database on air-water flow (Lucas et al., 2008, 2010) is used to validate model concepts for poly-dispersed flows but also closure models for bubble forces and bubble coalescence and breakup (e.g. Post-Guillen et al., 2009, Liao et al, 2010). While the available models for bubble forces provide an acceptable agreement with the experimental observations for a wide range of flow conditions the applicability of models for bubble coalescence and breakup is still limited (Krepper et al., 2008). First experiments using the wire-mesh sensor technology to investigate bubble condensation in an upwards vertical pipe were done in 2004. They clearly showed the effect of interfacial area density by comparison of experimental results for which only the initial bubble size distribution was modified by using different orifice sizes for bubble injection, but keeping the gas and liquid flow rates constant (Lucas and Prasser, 2007). Nevertheless these experiments had some preliminary character and some shortcomings due to the limited temperature measurement, the availability of only one wire-mesh sensor (not allowing to determine the gas velocity) and also due to the set pressure boundary condition. Learning from these tests, now new experiments are conducted. The new experiments base on the experimental setup used for the generation of the above mentioned air-water database (Lucas et al., 2010). Some extensions as described below were done to meet the requirements for measurements on flows with phase transfer.

2. DESCRIPTION OF THE EXPERIMENTS

2.1 The TOPFLOW facility

TOPFLOW is the acronym for **T**ransient tw**O P**hase **FLOW** test facility. It is designed for the generic and applied study of transient two-phase flow phenomena in the power and process industries. By

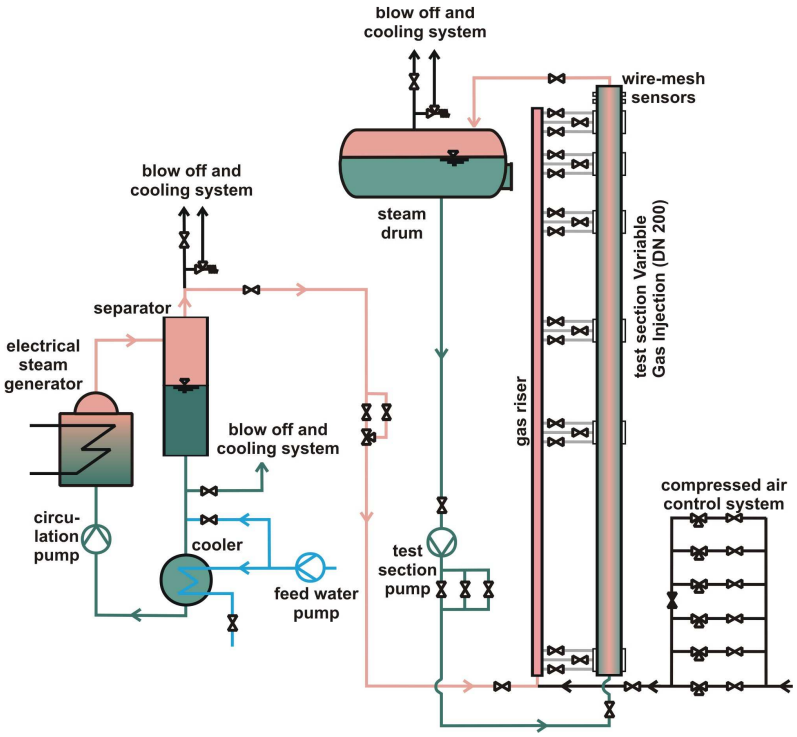

Fig. 1: The integration of the Variable Gas Injection test section in the TOPFLOW facility

applying innovative measuring techniques TOPFLOW provides data suitable for CFD code development and qualification. TOPFLOW allows to perform steam-water or air-water experiments. The facility was described in detail by Schaffrath et al. (2001) and Prasser et al. (2006). Additional information can be found at the TOPFLOW website (www.fzd.de/db/Cms?pNid=1003).

TOPFLOW can be operated at pressures up to 7 MPa and the corresponding saturation temperature of 286 °C. The maximum steam mass flow is about 1.4 kg/s, produced by a 4 MW electrical heater. The maximum saturated water mass flow rate through the vertical test section is 50 kg/s. Different test sections can be operated between the heat source (steam generator) and the heat sink (cooling systems). Fig. 1 shows a scheme of the integration of the test section loop in the TOPFLOW facility.

2.2 The Variable Gas Injection and the measuring procedure

As in previous experiments on steam bubble condensation (Lucas and Prasser, 2007) the Variable Gas Injection device is used, but modifications were done to improve the experimental procedure as well as to improve the quality of the data. The scheme of the new setup is shown at Fig. 2. The test section consists of a vertical steel pipe with an inner diameter of 195.3 mm and a length of about 8 m. The measuring equipment which consists of a pair of wire-mesh sensors and a lance with thermo-couples is located at the upper end of the test section. The extended device is equipped with seven gas injection units which allow to inject air or steam via orifices in the pipe wall. The gas injection via wall orifices offers the advantage that the two-phase flow can rise smoothly to the measurement plane, without being influenced by the feeder within the tube at other height positions. The injection devices are arranged almost logarithmically over the pipe length since the flow structure varies quite fast close to the gas injection mainly caused by the radial redistribution of the gas. Six of the gas injection modules consist of three injection chambers each. Two of the three chambers (the uppermost and the lowest) have 72 x 1 mm orifices. The middle chamber has 32 x 4 mm orifices, which is used to vary the initial bubble size distribution. For rotation–symmetric gas injection, all orifices per chambers are equally distributed over the circumference of the pipe. For the new condensation experiments an additional injection chamber with 1 mm orifices is installed as close to the measuring plane as possible (38 mm between gas injection and measurement plane of the first wire-mesh sensor in flow direction; L/D ~ 0.2). This was done to provide more detailed information on the injected steam bubbles. Only one injection chamber is activated for a single measurement. L/D is increased by using the steam injection chambers from "@" through "R" and "B" through "Q" for 1 and 4 mm injection respectively.

The liquid phase is supplied from the bottom of the test section by means of an isolating valve and a 90° bend. The test section pump (see Fig. 1) circulates the saturated water from the steam drum to the lower end of the variable gas injection. In addition cold water is injected through a mixing device at

the lower end of the test section. This allows to obtain a sub-cooling of the water of several Kelvin depending on the flow rates.

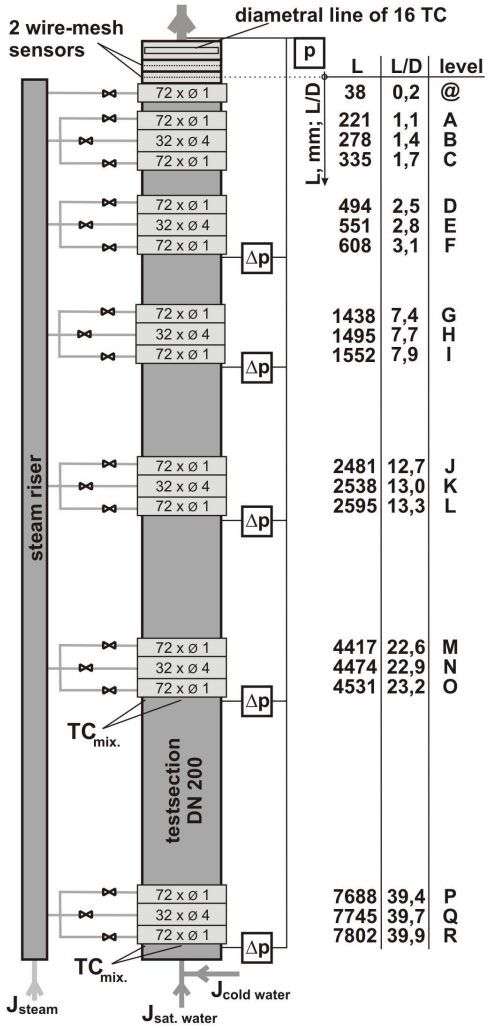

Fig. 2: Scheme of the test section Variable Gas Injection (from Lucas et al., 2010b)

In contrast to the previous experiments (Lucas and Prasser, 2007) the nominal pressure is now set at the position of the respectively activated injection chamber. Thus switching between different positions of the injection provides the same conditions like in case of a fixed location of the injection and shifting the measuring plane. This is especially important for the condensation experiments since the saturation temperature and by that also the sub-cooling depends on pressure. To adjust the pressure the absolute value is measured at the upper end of the test section. In addition the differential pressure between this measurement position and the position of the single gas injection is determined (see Fig. 2). After adjusting the pressure for the selected flow rates and for the position of the activated steam injection, the aspired sub-cooling has to be set up. The water temperature is measured by thermocouples, mounted in the saturated and the cold water pipes as well as in the Variable Gas Injection pipe below the injection levels R and O for the mixing temperature (see Fig. 2). The total water mass flow rate (saturated water from the loop and the additional cold water injection) and the water temperature are adjusted together finally to reach the aspired values.

2.3 Measuring techniques

Numerous papers were published in the past on the wire-mesh sensor technology (e.g. Prasser et al., 1998, 2001) and on experiments using the wire-mesh sensor (e.g. Lucas et al., 2010). For this reason here only the basic principle is presented. A wire-mesh sensor consists of two grids of parallel wires, which span over the measurement cross-section. The wires of both planes cross under an angle of 90°, but do not touch. Instead there is a vertical distance between the wires at the crossing points. At these points the conductivity is measured. According to the different conductivity of gas and water the phase present in the moment of the measurement at the crossing point can be determined. Many different types of wire-mesh sensors were built and successfully used during the last 15 years.

In the present case, two new developed high temperature wire-mesh sensors (Fig. 3) are employed. They are designed for an operational pressure up to 7 MPa and the corresponding saturation temperature of 286°C. Each plane of the sensors is composed of 64 x 64 wires that have a lateral pitch of 3 mm. The distance between the two grid levels is app. 3 mm. Due to thermal expansion it is necessary to stress each single wire by a spring. A disadvantage of the previous wire-mesh sensor design was the occurrence of leakages at high pressures. For this reason the present sensor seals each of the 128 wire electrodes with a single packing box. Inside these boxes employed a new synthetic material which allows the electrical and pressure insulation simultaneous up to high temperatures. Additionally, the packing boxes simplify the replacement of damaged wires. Furthermore the body of the sensor is designed modular. This feature reduces the weight of the sensor essential and simplifies the maintenance.

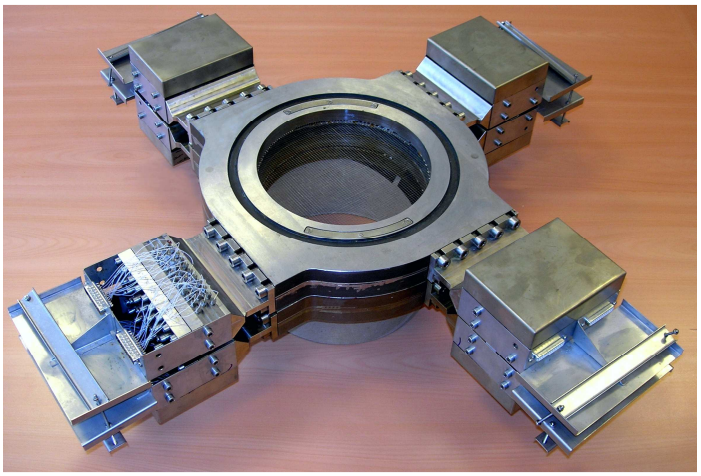

Fig. 3: High temperature wire-mesh sensors used in the present experiments

Measurements are done with a frequency of 2500 frames per second, i.e. 2500 pictures of the instantaneous gas distribution in the pipe cross section are obtained. The measuring time was 10 s, i.e. the result of one single measurement is a three-dimensional matrix of 64*64*25.000 values of the instantaneous local conductivity. By a calibration procedure a matrix of the instantaneous local volume void fraction with the same dimensions is calculated.

The 64*64*25.000 matrix of void fraction values can be visualized to provide an impression of flow characteristics. More important is the generation of quantitative data by using averaging procedures. Most important is the time averaging, which e.g. leads to time averaged two-dimensional gas volume fraction distributions in the pipe cross section. Due to the radial symmetry of the data the statistical error can be further lowered by an azimuthally averaging. To do this the cross section is sub-divided into 80 ring-shaped domains with equal radial width. The contribution of each mesh is calculated by weight coefficients obtained from a geometrical assignment of the fractions of a mesh belonging to these rings. In the result radial gas volume fraction profiles are obtained.

For the measurements two sensors were used which measurement planes have a distance of 42 mm. This allows to cross-correlate the gas volume fraction values of the two-planes for all mesh points which are located above each other. From the maxima of the cross-correlation functions the typical time shift of the local void fraction fluctuations can be determined. Since the distance between the measuring planes is known the local time averaged gas velocity can be calculated. The point-to-point two-dimensional gas velocity distributions in the pipe cross section are obtained in the results of this procedure. Again an azimuthally averaging is applied to obtain the radial profiles of the gas velocity. Please consider, that the second sensor is only used for the determination of the gas velocities. Due to the perturbing effect of the first sensor other data as especially bubble size distributions obtained from the second sensor would be distorted.

The next step of the data evaluation procedure is the identification of single bubbles. A bubble is defined as a region of connected gas-containing elements in void fraction matrix which is completely surrounded by elements containing the liquid phase. A complex procedure, described by Prasser et al. (2001), applies a filling algorithm combined with sophisticated stop criteria to avoid artificial combinations as well as artificial fragmentation of bubbles. In the result the same identification number is assigned to all volume elements which belong to the same bubble. Different bubbles receive different identification numbers. These numbers are stored in the elements of a second array. This array has the same dimension as the void fraction array. Combining the information from the void faction and bubble number arrays together with the radial profiles of the gas velocity characteristic data of the single bubbles as bubble volume, sphere equivalent bubble diameter, maximum circle equivalent bubble diameter in the horizontal plane, coordinates of the bubble centre of mass, moments characterizing asymmetries and others are obtained. Based on these data cross section and time averaged bubble size distributions and radial gas volume fraction profiles decomposed according to the bubble size are calculated. The bubble size distributions are defined volume fraction related, i.e. they present the volume fraction per width of a bubble diameter class (equivalent diameter of a sphere with the measured bubble volume V_b is considered).

In addition to the measurement of the two-phase flow characteristics by wire-mesh sensors also information on local temperatures is required. For this reason a lance of thermocouples is mounted

directly above the second wire-mesh sensor. It spans over the whole pipe diameter. The single positions of the thermocouples can be assigned to single measuring points of the wire-mesh sensor.

2.4 Test matrix

Measurements are done for 1, 2, 4 and 6.5 MPa pressure at the location of the gas injection and different levels of sub-cooling. The sub-cooling of the water is defined as difference between the saturation temperature which corresponds to the above mentioned nominal pressure and the temperature of the water arriving from below at the activated injection chamber. Downstream from the steam injection the sub-cooling decreases for two reasons: a) the water is heated by the condensing steam and b) the saturation temperature decreases together with the pressure.

Table 1: Test matrix

Point	J_L [m/s]	J_G [m/s]	ΔT [K]
1 MPa			
118	1.017	0.219	3.9, 5.0
138	0.405	0.534	4.7, 5.3, 6.3, 6.6, 7.2
140	1.017	0.534	3.7, 4.8, 5.0, 6.0
2 MPa			
118	1.017	0.219	3.7, 4.9, 6.0
138	0.405	0.534	4.8, 6.6, 8.7
140	1.017	0.534	3.2, 5.0, 6.8
4 Mpa			
118	1.017	0.219	2.7, 5.0, 7.2
138	0.405	0.534	2.6, 6.6, 12.6
140	1.017	0.534	2.6, 5.0, 7.6
6.5 MPa			
096	1.017	0.0898	2.5, 5.0, 7.1
116	0.405	0.219	2.9, 7.7, 12.5
118	1.017	0.219	2.5, 5.0, 7.4

There are limits for a reasonable sub-cooling. While heat losses over the experimental loop are quite small a sub-cooling results from the fact, that the steam drum (which serves as separator in the test loop - see Fig. 1) is located at a height position similar to the top of the test section. Since the saturated water is taken from the steam drum sub-cooling is obtained at the lower end of the test section. The maximum sub-cooling is determined in general by the maximum flow rate of the cold water injection. For most experiments a more restrictive limit is given by the fact, that at a too high sub-cooling, the steam vanishes along the flow path quite fast. One important intension of these experiments is to observe the evolution of the condensing flow along the pipe. For this reason at least for the upper most injection chambers down until level I (see Fig. 2) steam should arrive at the measuring plane.

The minimum sub-cooling is obtained, if no additional cold water is injected in case of steam injection at the lowest injection device (i.e. largest L/D, levels P, Q and R – see Fig. 2). If higher injection devices are activated (measurements for lower L/D ratios) the system pressure has to be slightly increased to obtain the nominal pressure at this position due to the influence of hydrostatic pressure. An increase of pressure in the steam drum leads also to an increase of the water temperature since saturation conditions are established there. For this reason also in this limiting case some cold water has to be mixed in if higher steam injection chamber are activated.

Table 1 shows the test matrix. Measurements were done for 3 different combinations of gas and liquid superficial velocities. The numbers of the points correspond to the general FZD test matrix for pipe flow (see e.g. Lucas et al., 2010). For 1, 2 and 4 MPa a superficial velocity of about 1 m/s for water (J_L) and about 0.53 m/s for the injected steam (J_G) were taken as reference point (140). To vary the flow rates measurements were also done with decreased steam flow rate (point 118, $J_G \sim 0.22$ m/s) and decreased water flow rate (point 138, $J_L \sim 0.4$ m/s). Due to the limitations in gas discharge from the orifices for 6.5 MPa lower steam flow rates are used. There are still ongoing experiments for 6.5 MPa. Also the data evaluation is not completed for this pressure. For this reason in the followings section only data from 1 to 4 MPa are presented.

3. RESULTS

In the result of the measurements an extensive database containing detailed information on the local interfacial structure and on temperatures was obtained. Of course not all the data can be presented in this paper, but general features and observations made are discussed. Some results of the experiments done at a pressure of 1 MPa were already presented by Lucas et al. (2010b). Two examples which give a qualitative impression of the void fraction distribution in the pipe are shown in Fig. 4. While the cross section averaged void fraction decreases due to condensation over all the pipe length in case of 6.8 K sub-cooling, re-evaporation occurs for large L/D for the two cases with lower sub-cooling. This behaviour is discussed more in detail in the following section.

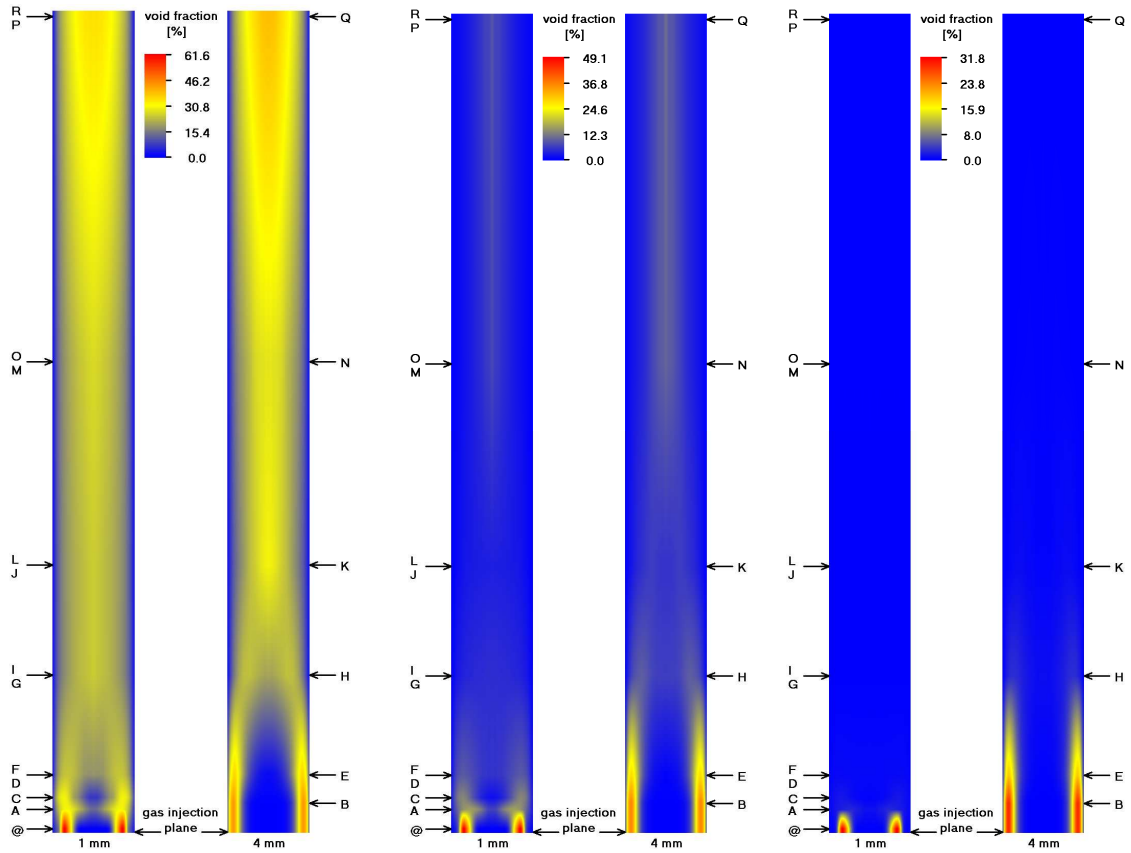

Fig. 4: Evolution of the void fraction along the pipe. Point 140 (J_L = 1.017 m/s, J_G = 0.534 m/s), 2 MPa, sub-cooling: 3.2 K (left), 5.0 K (middle) and 6.8 K (right)

3.1 Time and cross-section averaged void fraction

In case of high sub-cooling, that averaged void fraction continuously decreases along the pipe and the steam finally completely vanishes. Examples for the evolution of the void fraction are shown in Fig. 5 for two different pressure values. The volume flow rates of water and injected steam are the same in both cases. Although the sub-cooling is slightly larger in the 4 MPa case (7.6 K) the decrease of the void fraction is slightly slower compared to the 2 MPa case (sub-cooling 6.8 K). This is mainly due to the larger steam density. Also the influence of interfacial area density is clearly visible from the plots. Leaving all other parameter unchanged, the steam injection trough 1 mm orifices produces smaller bubbles compared to the 4 mm injection, i.e. the interfacial area density is larger. Consequently the condensation rate is larger in case of the 1 mm injection. For these cases with high sub-cooling the water temperature clearly remains lower than the saturation temperature at each position along the pipe.

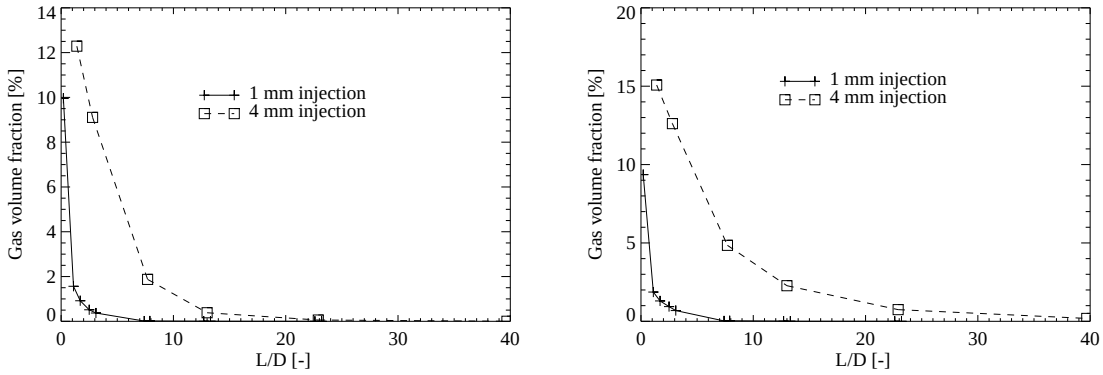

Fig. 5: Evolution of the cross section averaged void fraction along the pipe. Point 140 (J_L = 1.017 m/s, J_G = 0.534 m/s), left: 2 MPa and 6.8 K sub-cooling, right: 4 MPa and 7.6 K sub-cooling

The situation is different for cases with low sub-cooling. Fig. 6 presents as an example the measurement done at 2 MPa and 3.2 K sub-cooling. For L/D < 10…15 the void fraction again decreases. For larger L/D an increase of the void fraction is observed which is mainly caused by evaporation. Of course the decrease of pressure along the pipe leads to a slight expansion of the gas, but this effect is much smaller. Due to the decreasing pressure with increasing L/D also the saturation temperature decreases (see Fig. 6, right-hand side). On the other hand due to condensation of the injected steam there is an increase of the water temperature. Most of this increase is observed directly at the position of the steam injection. For this reason the sub-cooling measured for the smallest L/D is already much smaller than the set value. Starting from L/D = 10…15 saturation conditions are reached and evaporation occurs. In this case the water temperature should be slightly higher than the saturation temperature. This is not seen in Fig. 6 (right-hand side). This demonstrates the uncertainty of the temperature measurement. Also after careful calibration the error of the thermo-couple measurement is in the order of 1 K. As in the example shown in Fig. 6 also in all other cases with re-evaporation the curves of the saturation temperature and the measured water temperatures are parallel.

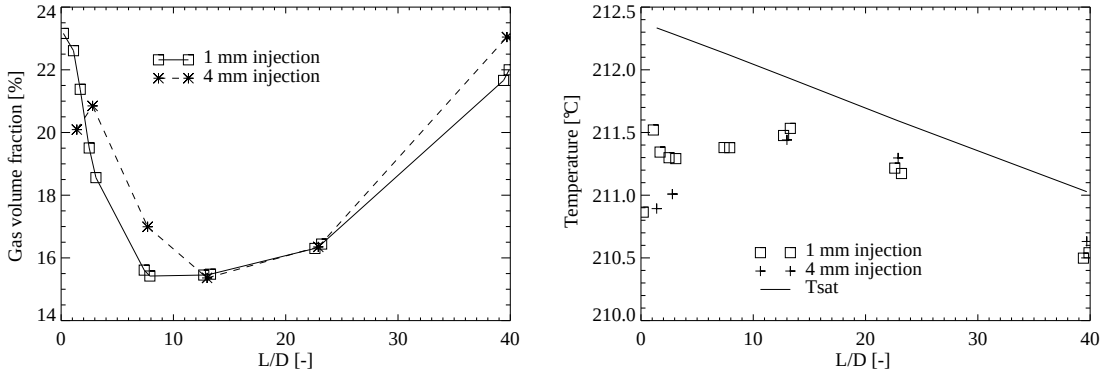

Fig. 6: Evolution of the cross section averaged void fraction (left) and averaged temperature (right) along the pipe. Point 140 (J_L = 1.017 m/s, J_G = 0.534 m/s), 2 MPa and 3.2 K sub-cooling

The evolution of the averaged void fraction along the pipe for decreased steam and water flow rates and lowest sub-cooling values measured are shown in Fig. 7. The results are compared for different pressure values. Figs. 5 to 7 show, that the interfacial area density is important as long as a clear sub-cooling is obtained. In contrast for conditions close to the saturation the dynamics of the phase transfer process are of less importance.

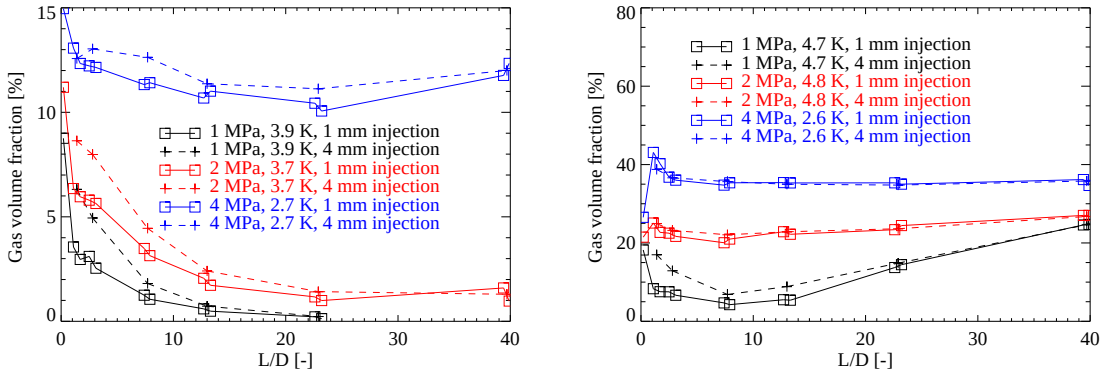

Fig. 7: Evolution of the cross section averaged void fraction along the pipe. left: point 118 (J_L = 1.017 m/s, J_G = 0.219 m/s), right: point 138 (J_L = 0.405 m/s, J_G = 0.534 m/s)

3.2 Radial profiles

Since the steam is injected from the pipe walls the maximum of the radial void fraction profiles is found in the outer region of the pipe for small L/D. During the condensation process the bubbles migrate towards the pipe centre as shown in Fig. 8. The spreading of the steam over the pipe cross section gives useful data for the validation of models for lateral bubble forces. Due to the buoyancy effects the radial void fraction profile also influences the radial velocity profile. An example is also shown in Fig. 8.

Obviously there is for all cases an intensive radial mixing of the liquid. For none of the experiments a pronounced radial profile of the temperature was observed. The temperature differences obtained from the single thermo couples distributed over the pipe radius are within the error level of the temperature measurement.

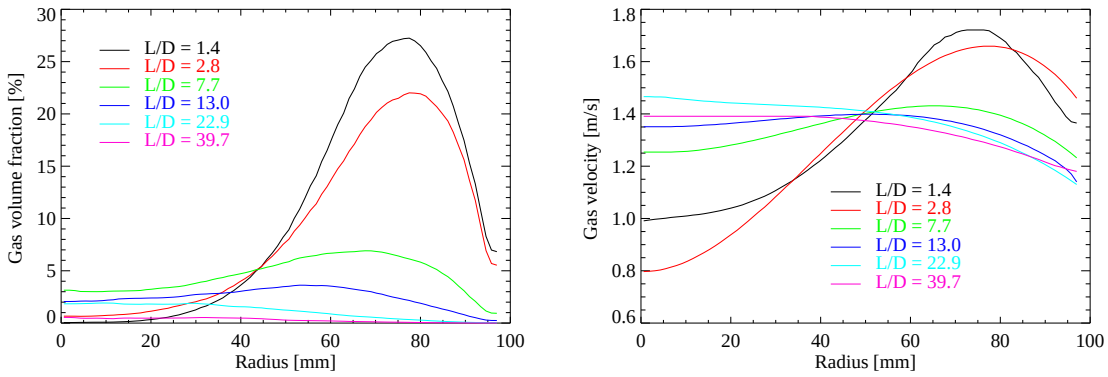

Fig. 8: Radial profiles of the void fraction (left) and the gas velocity (right). Point 140 (J_L = 1.017 m/s, J_G = 0.534 m/s), 4 MPa and 7.6 K sub-cooling, 4 mm injection

The new steam injection chamber with 1mm orifices located at L/D = 0.2 below the wire-mesh sensor gives some insight in the flow situation close to the injection. As discussed by Lucas et al. (2010b) for the 1 MPa experiments also for higher pressure the radial velocity profiles are characterized at this position by a steep decrease of the gas velocity as demonstrated in Fig. 9 (right-hand side). The radial position of this steep decrease corresponds to the position of the maximum of the radial void fraction distribution (Fig. 9, left-hand side). The radial steam injection leads to a strong vortex. At the centre of this vortex the steep decrease is observed and the steam collects at the centre of this vortex. Due to the larger radial momentum the centre of the vortex is at a lower radial position for point 140 compared to

point 118. Also the height of the step of the velocity profile is slightly larger for the 4 MPa cases compared to the 2 MPa ones.

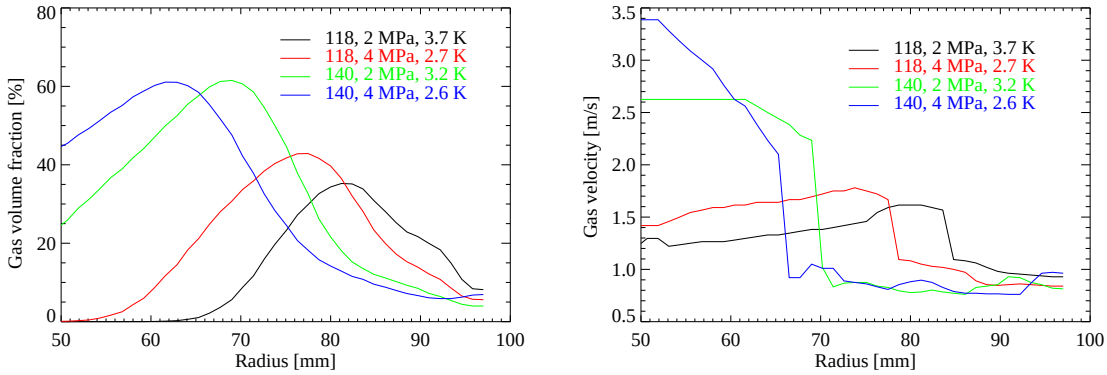

Fig. 9: Radial profiles of the void fraction (left) and the gas velocity (right) at L/D = 0.2. (J_L = 1.017 m/s, point 118: J_G = 0.219 m/s, point 140: J_G = 0.534 m/s)

3.3 Effects of bubble sizes

Bubble size distributions are calculated from the raw data as described in section 2.3. They present the gas volume fraction represented by each bubble class. Fig. 10 gives an example for the different bubble size distributions resulting from the 1 mm and 4 mm injection. Much larger primary bubbles are generated by the 4 mm injection. For the 1 mm injection the condensation process is superposed by bubble coalescence for small L/D. The size of the largest bubbles first increases until L/D ~ 7.4. The maximum of the distribution decreases for L/D > 2.5. For the largest L/D measured (~ 40) the bubble size distributions are similar for both injections. From Fig 7 (left side, red curve) can be seen, that some re-evaporation occurs at L/D ~ 40.

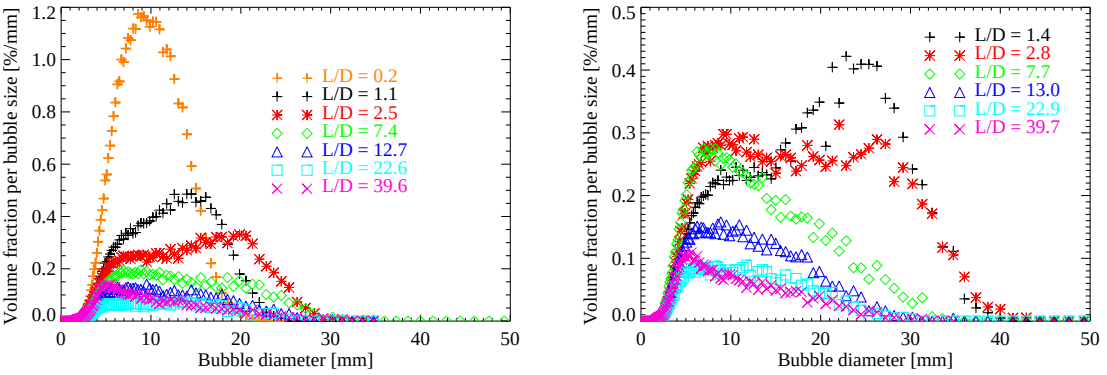

Fig. 10: Bubble size distributions for point 118 (J_L = 1.017 m/s, J_G = 0.219 m/s), 2 MPa, sub-cooling 3.7 K 1 mm injection (left) and 4 mm injection (right)

Fig. 11 shows bubble size distributions for a case with relatively weak condensation at low L/D and evaporation for large L/D (see Fig. 6) and a case with strong condensation all along the pipe (see Fig. 5, right-hand side). In the first case there are only slight changes of the bubble size distribution observed along the pipe, while in the condensation case a continuous shift of the distribution towards smaller bubbles is found.

One example for radial gas volume fraction profiles, decomposed according to the bubble size is given in Fig. 12. According to the lift force correlation by Tomiyama (2002) the critical diameter at which

the lift force changes its sign should be equal 4.4 mm for steam-water at 2 MPa. Indeed the experimental results show wall peak for bubbles less then 4.5 mm and a core peak for larger ones.

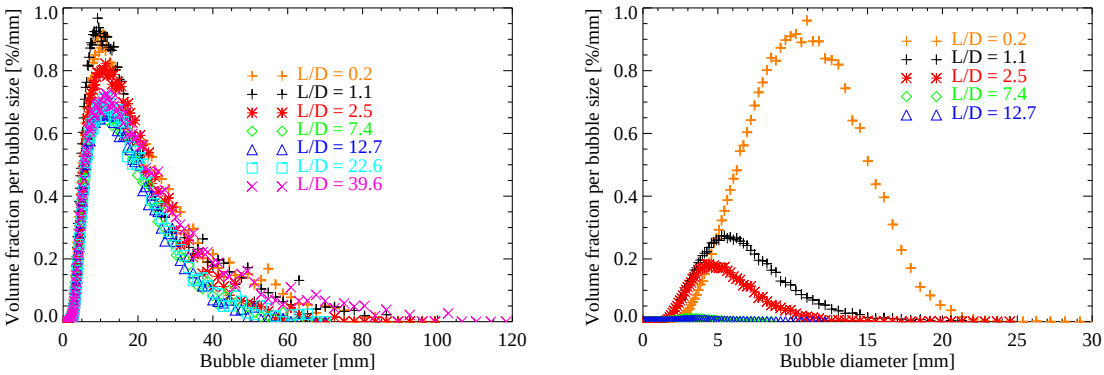

Fig. 11: Bubble size distributions for point 140 (J_L = 1.017 m/s, J_G = 0.534 m/s), 1 mm injection, 2 MPa, sub-cooling 3.2 K (left), 4 MPa, sub-cooling 7.6 K (right)

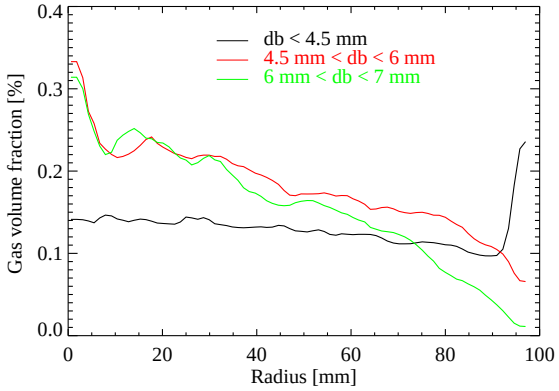

Fig. 12: Radial gas volume fraction profiles formed by bubbles of defined size ranges, point 118 (J_L = 1.017 m/s, J_G = 0.219 m/s), 2 MPa, sub-cooling 3.7 K, 4 mm injection, L/D = 39.7

3.4 Uncertainties of the measurements

Systematic as well as statistic error have to be considered. In general the number of measured bubbles is very high leading for all the presented data to a statistic error which is much smaller compared to possible systematic errors. This can also be seen from the flatness of the curves. An exception is the data decomposed according to the radial position and the bubble size. The fluctuations of the curves shown in Fig. 12 result from statistics. The error of the temperature measurement is about 1K.

Several investigations were done regarding systematic errors of the wire-mesh sensor measurements. Most important is the interaction between the bubbles and the sensor. Due to the lower surface tension this effect should be weaker for steam-water flows as investigated in this work compared to air-water flow at ambient conditions. Comparative measurements with gamma radiography of an air/water flow showed that the deviations between wire-mesh sensor and gamma measurement are limited to ± 5 % (Prasser 2000). The radiography of a steam/water flow at atmospheric pressure confirmed this statement (Manera et al. 2001). Differences in the absolute void fraction were determined in a comparison to X-ray tomography (Prasser et al. 2005) for a bubbly flow in the range of ± 1 % and for slug flow a systematic underestimation of approx. - 4 % was observed. Comparative measurements with a high-speed camera are available to estimate the measurement error for the determination of the volume equivalent bubble diameter. The investigations were performed in a transparent flow channel with air/water flows with different bubble sizes. Prasser et al. (2001) demonstrated that only bubbles with a diameter larger ~ 2 mm can be recorded due to the limited spatial resolution in case of a wire-mesh sensor with a pitch of the wires of 3 x 3 mm. In addition, the comparisons between the data of the wire-mesh sensor and the high-speed camera showed that the volume equivalent diameter is measured at superficial water velocities of > 0.2 m/s with an accuracy of ± 20 %. The data of an extensive air-water test series were used to compare air volume flow rates obtained from the measured void fraction and gas velocity profiles with the set values. An

overestimation up to about 20 % (relative error) was observed for the measurements on bubbly flows at low void fraction (Lucas et al., 2010b).

4. CONCLUSIONS

CFD-grade data suitable for the validation of CFD approaches for poly-dispersed flows as well as corresponding closure models for mass, momentum and energy transfer between the phases are obtained in a new measuring series at the TOPFLOW facility of Forschungszentrum Dresden-Rossendorf. Condensing upward vertical pipe flow is investigated for pressure values of 1, 2, 4 and 6.5 MPa. Steam and water flow rates and the level of sub-cooling were also varied. Due to decreasing hydrostatic pressure along the pipe in some cases also re-condensation was obtained. The database presently comprises radial gas volume fraction profiles, radial profiles of the gas velocity, bubble size distributions, radial volume fraction profiles decomposed according to the bubble size and temperature distributions. The data are presently used to validate the extensions of the Inhomogeneous MUSIG model for phase transfer recently implemented into CFX (Schmidtke et al., 2010).

ACKNOWLEDGEMENTS

This work is carried out in the frame of a current research project funded by the German Federal Ministry of Economics and Technology, project number 150 1329. The authors like to thank all members of the TOPFLOW team who contributed to the successful performance of these experiments.

REFERENCES

D. Bestion, D. Lucas, M. Boucker, H. Anglart, I. Tiselj, Y. Bartosiewicz, “Some lessons learned from the use of two-phase CFD for nuclear reactor thermalhydraulics”, *Proceedings of the 13th International Topical Meeting on Nuclear Reactor Thermal Hydraulics (NURETH-13)*, Kanazawa, Japan, 27.9. – 2.10.2009, Paper N13P1139 (2009).

D.A Drew, R.T. Lahey Jr., R.T., “Application of general constitutive principles to the derivation of multidimensional two-phase flow equation”, *Int. J. Multiphase Flow*, 5, 243–264 (1979).

T. Frank, P. Zwart, E. Krepper, H.-M. Prasser, D. Lucas, “Validation of CFD models for mono- and polydisperse air-water two-phase flows in pipes”, *Nucl. Eng. and Design*, 238, 647-659, (2008).

M. Ishii, K. Mishima, “Two fluid model and hydrodynamic constitutive relations”, *Nucl. Eng. Des.*, 82, 107–126 (1984).

E. Krepper, D. Lucas, H.-M. Prasser, “On the modelling of bubbly flow in vertical pipes”, *Nucl. Eng. and Design*, 235, 597-611 (2005).

E. Krepper, D. Lucas, T. Frank, H.-M. Prasser, P. Zwart, “The inhomogeneous MUSIG model for the simulation of polydispersed flows”, *Nucl. Eng. and Design*, 238, 1690-1702, (2008).

Y. Liao, D. Lucas, “Influence of Turbulence Models on the Bubble Coalescence and Breakup Behavior in Poly-disperse Gas-Liquid Flows”, *NUTHOS-8, International Topical Meeting on Nuclear Thermal-Hydraulics, Operation and Safety*, Shanghai, China, October 10-14, (2010).

D. Lucas, E. Krepper, H.-M. Prasser, “Prediction of radial gas profiles in vertical pipe flow on basis of the bubble size distribution”, *Int. J. of Thermal Sciences*, 40, 217-225, (2001).

D. Lucas, E. Krepper, H.-M. Prasser, “Use of models for lift, wall and turbulent dispersion forces acting on bubbles for poly-disperse flows”, *Chem. Science and Eng.*, 62, 4146-4157, (2007).

D. Lucas, H.-M. Prasser, Steam bubble condensation in sub-cooled water in case of co-current vertical pipe flow, *Nucl. Eng. and Design*, 237, 497-508, (2007).

D. Lucas, M. Beyer, J. Kussin, P. Schütz, “Benchmark database on the evolution of two-phase flows in a vertical pipe”, *XCFD4NRS, Experiments and CFD Code Applications to Nuclear Reactor Safety*, 10.-12.09.2008, Grenoble, France, (2008).

D. Lucas, M. Beyer, T. Frank, P. Zwart, A. Burns, "Condensation of Steam Bubbles Injected into Sub-Cooled Water", *Proceedings of the 13th International Topical Meeting on Nuclear Reactor Thermal Hydraulics (NURETH-13)*, Kanazawa, Japan, 27.9. – 2.10.2009, Paper N13P1097 (2009).

D. Lucas, M. Beyer, L. Szalinski, P. Schütz, "A new database on the evolution of two-phase flows in a large vertical pipe", *Int. J. of Thermal Sciences*, 49, 664-674 (2010).

D. Lucas, M. Beyer, L. Szalinski, "Experimental investigations on the condensation of steam bubbles injected into sub-cooled water at 1 MPa", *Multiphase Science and Technology*, accepted, (2010b).

A. Manera, H.-M. Prasser, T.H.J.J. Van der Hagen, R.F. Mudde, M. de Kruijf, "A comparison of void-fraction measurements during flashing-induced instabilities obtained with a wire-mesh sensor and a gamma-transmission set-up", *4th Int. Conf. on Multiphase Flow*, New Orleans, USA, paper 436, (2001).

D. Post Guillen, J.K. Shelley, S.P. Antal, E.A. Tselishcheva, M.Z. Podowski, Michael Z., D. Lucas, M. Beyer, "Optimization of a two-fluid hydrodynamic model of churn turbulent flow", *Proceedings of the17th International Conference on Nuclear Engineering, ICONE 17*, 12.-16.07.2009, Brussels, Belgium, (2009).

H.-M. Prasser, A. Böttger, J. Zschau, "A new electrode-mesh tomograph for gas/liquid flows", *Flow Measurement and Instrumentation*, 9, 111 – 119, (1998).

H.-M. Prasser, "High-speed measurement of the void fraction distribution in ducts by wire-mesh sensors", *Proceedings of the International Meeting on Reactor Noise*, Oct. 11-13, 2000, Athens, Greece, proc. on CD-ROM, paper_7_1.doc, (2000).

H.-M. Prasser, D. Scholz, C. Zippe, "Bubble size measurement using wire-mesh sensors", *Flow Measurement and Instrumentation*, 12, 299-312, (2001).

H.-M. Prasser, M., Misawa, I. Tiseanu, I., "Comparison between Wire-mesh sensor and ultra-fast X-ray tomograph for an air/water flow in a vertical pipe" *Flow Meas. and Instr*., 16, 73-83 (2005).

H.-M. Prasser M. Beyer, H. Carl, A. Manera, H. Pietruske, P. Schütz, F.-P. Weiß, "The multipurpose thermal-hydraulic test facility TOPFLOW: an overview on experimental capabilities, instrumentation and results", *Kerntechnik*, 71, 163-173, (2006).

H.-M. Prasser, M. Beyer, H. Carl, S. Gregor, D. Lucas, H. Pietruske, P. Schütz, F.-P. Weiss, "Evolution of the structure of a gas–liquid two-phase flow in a large vertical pipe", *Nucl. Eng. and Design*, 237, 1848–1861 (2007).

A. Schaffrath, A.-K. Krüssenberg, F.-P. Weiß, E.-F. Hicken, M. Beyer, H. Carl, H.-M., Prasser, J. Schuster, P. Schütz, M. Tamme, M., "TOPFLOW - a new multipurpose thermalhydraulic test facility for the investigation of steady state and transient two-phase flow phenomena", *Kerntechnik*, 66, 209-212, (2001).

M. Schmidtke, D. Lucas, E. Krepper, M.Beyer, C. Lifante, "Steam bubble condensation in co-current sub-cooled water in a vertical pipe – experiments and CFD simulation", *7th International Conference on Multiphase Flow, ICMF 2010*, Tampa, Fl, May 30 – June 4, 2010.

L. Szalinski, M. Da Silva, S. Thiele, M. Beyer, D. Lucas, U. Hampel, V. Hernandez Perez, L.A. Abdulkareem, B.J. Azzopardi, "Comparison study of gas-oil and gas-water two-phase flow in vertical pipes", *Chem. Science and Eng*., doi:10.1016/j.ces.2010.03.024, (2010).

A. Tomiyama, H. Tamai, I. Zun, S. Hosokawa, "Transverse migration of single bubbles in simple shear flows", *Chem. Eng. Sci.*, 57, 1849-1858 (2002).